Assessment of correlation energies based on the random-phase approximation

2012 New J. Phys. 14 043002

(http://iopscience.iop.org/1367-2630/14/4/043002)

New Journal of Physics
The open-access journal for physics

Assessment of correlation energies based on the random-phase approximation

Joachim Paier[1,7], Xinguo Ren[2,3,7], Patrick Rinke[2,3,7], Gustavo E Scuseria[4,5], Andreas Grüneis[6,7], Georg Kresse[6] and Matthias Scheffler[2,3]

[1] Institut für Chemie, Humboldt-Universität zu Berlin, Unter den Linden 6, 10099 Berlin, Germany
[2] Fritz-Haber-Institut der Max-Planck-Gesellschaft, Faradayweg 4–6, D-14195 Berlin, Germany
[3] European Theoretical Spectroscopy Facility (ETSF)
[4] Department of Chemistry, Rice University, Houston, TX 77005, USA
[5] Department of Physics and Astronomy, Rice University, Houston, TX 77005, USA
[6] Faculty of Physics and Center for Computational Materials Science, Universität Wien, Sensengasse 8/12, A-1090 Wien, Austria
E-mail: joachim.paier@chemie.hu-berlin.de, ren@fhi-berlin.mpg.de, rinke@fhi-berlin.mpg.de and ag618@cam.ac.uk

New Journal of Physics **14** (2012) 043002 (23pp)
Received 1 November 2011
Published 2 April 2012
Online at http://www.njp.org/
doi:10.1088/1367-2630/14/4/043002

Abstract. The random-phase approximation to the ground state correlation energy (RPA) in combination with exact exchange (EX) has brought the Kohn–Sham (KS) density functional theory one step closer towards a universal, 'general purpose first-principles method'. In an effort to systematically assess the influence of several correlation energy contributions beyond RPA, this paper presents dissociation energies of small molecules and solids, activation energies for hydrogen transfer and non-hydrogen transfer reactions, as well as reaction energies for a number of common test sets. We benchmark EX + RPA and several flavors of energy functionals going beyond it: second-order screened exchange (SOSEX), single-excitation (SE) corrections, renormalized single-excitation (rSE) corrections and their combinations. Both the SE correction and the SOSEX contribution to the correlation energy significantly improve on the notorious tendency of EX + RPA to underbind. Surprisingly, activation

[7] Authors to whom any correspondence should be addressed.

energies obtained using EX + RPA based on a KS reference alone are remarkably accurate. RPA + SOSEX + rSE provides an equal level of accuracy for reaction as well as activation energies and overall gives the most balanced performance, because of which it can be applied to a wide range of systems and chemical reactions.

Contents

1. Introduction

In the context of first principles electronic structure theory, 'exact-exchange plus correlation in the random-phase approximation (EX + RPA)' [1, 2] has recently attracted renewed and widespread interest [3–30]. In practice, the RPA calculations are most often performed in a non-self-consistent manner where the exchange-correlation (xc) energy contributions are evaluated with input orbitals corresponding to an approximate, usually semilocal xc energy functional. The great interest in EX + RPA is largely due to its three attractive features: (i) the exact-exchange energy (EX) cancels the spurious self-interaction error present in the Hartree energy, (ii) the RPA correlation energy is fully non-local and includes long-range van der Waals (vdW) interactions automatically and seamlessly [31] and (iii) EX + RPA is applicable to small-gap or metallic systems by summing up the sequence of 'ring' diagrams to infinite order. The latter is in contrast to order-by-order perturbation theories (e.g. second-order Møller–Plesset (MP2) [32]) that break down for systems with zero gap. Moreover, one can interpret the RPA as an approach that screens the non-local exchange, resulting in a frequency-dependent non-local screened exchange interaction, as opposed to conventional or global hybrid functionals where the parameters that reduce or 'screen' the EX contribution are fixed and system independent [33–35]. Such a system-independent 'screening' is expected to be unreliable for metals or wide-gap insulators, where non-local exchange is almost entirely screened (metals) or prevails to a large extent (insulators).

While a critical assessment of EX + RPA is emerging [5–10, 12–26, 28], some shortcomings have been known for a while. Total energies are typically significantly overestimated [3, 9, 11, 28, 36, 37], which is caused by an overestimation of the correlation energy at the short range. Binding energies, on the other hand, show a tendency to be underestimated [3, 7, 8, 12, 13, 16, 17, 25, 38]. Moreover, the RPA correlation energy is not self-correlation-free [9, 37, 39].

It has been demonstrated that overestimation of the absolute correlation energy can be almost entirely removed by adding a second-order screened exchange (SOSEX) term [36, 37, 39]. For one-electron systems the self-interaction error in EX + RPA is exactly canceled by adding this term [37, 39]; however, for systems with more than one electron, a many-electron self-interaction error [40, 41] prevails [39]. The SOSEX can also be interpreted as a correction to the RPA correlation energy that can be included to *approximately* restore the antisymmetry of the many-electron description [39]. Furthermore, SOSEX improves binding energies, although a sizeable underestimation persists [9, 36, 37, 39, 42, 43]. The underbinding problem can also be alleviated, in particular for weakly interacting systems, by adding a correction deriving from single excitations (SEs) [25] to EX + RPA built on a reference state obtained from the Kohn–Sham (KS) density functional theory (DFT). This suggests that RPA(+SOSEX) yields good estimates for the correlation energy, but errors in the exchange energy are sizeable if KS orbitals are used to evaluate the EX.

In light of these observations it is timely to extend the critical assessment of EX + RPA to a wider class of systems and to consider combinations of the corrections suggested before. In this paper, we will address this objective by performing benchmark calculations for atomization energies on an appreciable test set of archetypal insulating solids and small molecules [44–47] as well as reaction and activation energies for hydrogen and non-hydrogen transfer reactions [48, 49]. The schemes we include are EX + RPA based on KS-DFT reference states, and those beyond EX + RPA by adding corrections from SE or SOSEX individually, or from both of them. In addition we will also assess the hybrid-type schemes [25] where one replaces the total energy at the EX level evaluated with KS-DFT orbitals by that evaluated with Hartree–Fock (HF) orbitals, as an effective way to approximate the SE contribution [50]. The second-order SE correction can diverge when the gap between occupied and virtual states closes, with detrimental effects for the description of the transition states in chemical reactions. As discussed briefly in [25], including higher-order terms in the spirit of RPA permits a resummation of the SE correction, as will be demonstrated in section 2.3. This so-called renormalized SE (rSE) is well behaved and is included in our benchmark tests.

The paper is organized as follows. Sections 2 and 3 briefly summarize the important aspects of the underlying theory and the computational parameters of our work. Results on molecular and solid-state atomization energies as well as reaction energies and barrier heights are presented in section 4 before we draw conclusions in section 5.

2. Theory

2.1. Basics of random-phase approximation (RPA)

In order to properly position the methods applied in the present work within the formal framework of DFT, we briefly recapitulate essential equations and outline the structure of the functionals used. Currently, for total energy calculations, RPA-based functionals usually

use either KS-DFT reference states, i.e. single-particle wavefunctions and eigenvalues or generalized KS (GKS) [51] reference states, to compute the *non-local* EX energy as well as the *non-local* correlation energy [3, 5, 7]. In this context, the total energy is defined as

$$E[n] = T_s[\{\phi_i\}] + E_H[n] + E_{ext}[n] + E_x[\{\phi_i\}] + E_c[\{\phi_i\}], \tag{1}$$

where the terms deriving from the potential contributions in the Hamiltonian, E_H, the electrostatic Hartree or Coulomb energy, and E_{ext}, the (external) electron–ion interaction, depend on the local density, whereas the last two terms, EX energy E_x and correlation energy E_c, are nonlocal contributions. Note that the KS kinetic energy, in analogy to the EX energy, is not an explicit functional of the density, but rather of the KS orbitals. The non-locality in E_x is due to the nonlocal exchange operator acting on each (occupied) orbital $\phi_{i\sigma}(\mathbf{r})$ associated with spin σ and its well-known dependence on the (nonlocal) reduced one-particle density matrix $\rho_\sigma(\mathbf{r}, \mathbf{r}') = \sum_j^{occ} \phi_{j\sigma}(\mathbf{r})\phi^*_{j\sigma}(\mathbf{r}')$ reads

$$E_{x,\sigma} = -\frac{e^2}{2} \iint \frac{|\rho_\sigma(\mathbf{r}, \mathbf{r}')|^2}{|\mathbf{r} - \mathbf{r}'|} \, d^3\mathbf{r} \, d^3\mathbf{r}'. \tag{2}$$

In contrast to the optimized effective potential (OEP) method [52–54], in the HF theory the exchange operator is fully nonlocal, and the action of the exchange operator on a single-particle wavefunction (i.e. orbital) depends on the value of that very orbital throughout the entire space (see [55]). Note that the correlation energy E_c is a functional of both occupied and unoccupied eigenstates and requires knowledge of the associated eigenenergies as well (see below). However, both E_x and E_c are *implicit* functionals of the electron density n (see, e.g., [56]). Recent work pursuing the construction of a *local* RPA correlation potential is presented in [57–62]. Work in this direction is of great value, since it ultimately enables calculations of self-consistent RPA correlation energies staying rigorously within the KS-DFT picture.

The RPA correlation energy can be conveniently derived from (i) perturbation theory or (ii) from the adiabatic-connection fluctuation-dissipation (ACFD) theorem [63–65]. Fundamental to the formalism is the adiabatic connection between the Hamiltonian $\hat{H}$ of an *interacting* many-electron system and the corresponding *non-interacting* KS Hamiltonian $\hat{H}_{KS}$. Formally, both systems may be simultaneously described by a coupling constant-dependent Hamiltonian $\hat{H}(\lambda)$, with λ being the coupling constant or the scaling factor in the electron–electron interaction, $v_\lambda = \lambda v(\mathbf{r} - \mathbf{r}')$. The electrons move in a λ-dependent external potential $v^\lambda_{ext}(\mathbf{r})$. Note that the ground-state density of $\hat{H}(\lambda)$ for all $\lambda \in [0, 1]$ is constant and is equal to the physical ground-state density $n(\mathbf{r})$, i.e. the ground-state density of the real system. $\hat{H}(\lambda = 1)$ is the physical many-electron Hamiltonian with $v_{\lambda=1}(\mathbf{r}) = v_{ext}(\mathbf{r})$, and $\hat{H}(\lambda = 0)$ is the KS Hamiltonian with $v_{\lambda=0}(\mathbf{r}) = v_{KS}(\mathbf{r}) = v_{ext}(\mathbf{r}) + v_H(\mathbf{r}) + v_{xc}(\mathbf{r})$. $v_H(\mathbf{r})$ is the electrostatic Hartree potential and $v_{xc}(\mathbf{r})$ is the xc potential. Within ACFD, the *exact* KS correlation energy can be written as

$$E_c = -\int_0^\infty \frac{du}{2\pi} \int_0^1 d\lambda \int d\mathbf{r} \int d\mathbf{r}', \{v(\mathbf{r} - \mathbf{r}') \times (\chi_\lambda(\mathbf{r}, \mathbf{r}'; iu) - \chi_0(\mathbf{r}, \mathbf{r}'; iu))\}. \tag{3}$$

Here $v(\mathbf{r} - \mathbf{r}') = 1/|\mathbf{r} - \mathbf{r}'|$ is the bare Coulomb interaction kernel, and χ_0 is the KS independent-particle response function at imaginary frequencies iu,

$$\chi_0(\mathbf{r}, \mathbf{r}'; iu) = 2 \sum_i^{occ} \sum_a^{unocc} \frac{\phi^*_i(\mathbf{r})\phi_a(\mathbf{r})\phi^*_a(\mathbf{r}')\phi_i(\mathbf{r}')}{iu + \varepsilon_i - \varepsilon_a} + \text{c.c.}, \tag{4}$$

where c.c. denotes the 'complex conjugate' and the prefactor 2 accounts for the spin degeneracy in closed-shell systems. In equation (3), χ_λ is the density–density response function of the 'intermediately' interacting many-electron system employing a scaled Coulomb potential v_λ. We adhere to the commonly used notation of $i, j, \ldots$ being occupied i.e. hole KS states and $a, b, \ldots$ being unoccupied or virtual, particle states. In principle, a Dyson-type integral equation [66] has to be solved for χ_λ,

$$\chi_\lambda = \chi_0 + \chi_0 \, (v_\lambda + f_{\mathrm{xc}}^\lambda) \, \chi_\lambda, \tag{5}$$

with f_{xc}^λ being the xc kernel, i.e. the functional derivative of the xc potential with respect to the density. Within RPA, $f_{\mathrm{xc}} = 0$, i.e. using many-body terminology [67], the so-called vertex corrections are not included in the response function χ or equivalently in the screening of the Coulomb interaction. Solving equation (5) for χ_λ with $f_{\mathrm{xc}}^\lambda = 0$ corresponds to the diagrammatic resummation of ring graphs [36, 68] to infinite order. In passing, we note that, working within RPA, equation (5) can be rearranged to

$$\chi_\lambda = (1 - \chi_0 v_\lambda)^{-1} \cdot \chi_0 = [1 + \chi_0 v_\lambda + \chi_0 v_\lambda \chi_0 v_\lambda + \cdots] \cdot \chi_0, \tag{6}$$

reflecting the above-mentioned summation of the (screened) Coulomb interaction up to infinite order in $\chi_0 v_\lambda$. As will be seen later, equation (6) resembles the CC amplitude equations where the so-called particle–particle, particle–hole and hole–hole ladder terms have been removed (see equation (17)). Starting from equation (6), the λ-integral is readily done and the final expression for the RPA correlation energy reads

$$E_c^{\mathrm{RPA}} = \int_0^\infty \frac{\mathrm{d}u}{2\pi} \mathrm{Tr}\{\ln(1 - \chi_0(\mathrm{i}u)v) + \chi_0(\mathrm{i}u)v\}. \tag{7}$$

2.2. From coupled-cluster theory to RPA and RPA+ second-order screened exchange (SOSEX)

From a DFT purist's point of view, the previously outlined ACFD terminology for the RPA is certainly the most consistent way to classify 'RPA' as a correlation energy *functional* to the many-electron ground state. An alternative formulation of the RPA may be motivated starting from many-body theory. Many-body or equivalently field-theoretical diagrammatic techniques originally developed in quantum electrodynamics and nuclear physics [69] have been applied to the homogeneous electron gas as well as finite systems such as atoms and molecules for several decades already. For systems that are not strongly correlated, the most successful diagrammatic, partial summation technique (see [56] and [70]) is the coupled-cluster (CC) expansion of the many-electron wavefunction. The CC expansion to the homogeneous electron gas has been applied by Freeman [36], Kümmel, Lührmann and Zabolitzky [71] and Bishop and Lührmann [72, 73]. The same CC expansion techniques are indispensable ingredients for highly accurate molecular calculations. Here, Čížek [74, 75], Paldus *et al* [76] and Bartlett and Purvis [77] have been pioneers, to name a few. A more complete list of references can be found in the recent review article by Bartlett and Musiał [70].

The CC expansion relies on the ansatz for the many-electron wavefunction, $|\Psi\rangle$,

$$|\Psi\rangle = \mathrm{e}^{\hat{T}} |\Phi\rangle, \tag{8}$$

to generate the exact ground state from the ground state $|\Phi\rangle$ of the reference system commonly within the HF approximation. Note that $\hat{T}$ may be represented by a sum of single, double and higher-order excitation operators, generating, in a similar way to configuration

interaction (CI) techniques, singly, doubly substituted determinants based on the HF reference wavefunction $|\Phi\rangle$. However, the CC expansion is distinct from CI by virtue of the exponential ansatz used in CC expansions (equation (8)) for the wavefunction $|\Psi\rangle$, with

$$e^{\hat{T}} = 1 + \hat{T} + \frac{1}{2!}\hat{T}^2 + \frac{1}{3!}\hat{T}^3 + \cdots, \tag{9}$$

introducing so-called disconnected products of excitations responsible for the size-extensivity of the CC correlation energy [78].

In coupled-cluster doubles theory (CCD), the excitation operator corresponds to a double excitation operator only, where

$$\hat{T} \equiv \hat{T}_2 \quad \text{with} \tag{10}$$

$$\hat{T}_2|\Phi\rangle = \sum_{i<j}^{N_{\text{occ.}}} \sum_{a<b}^{N_{\text{virt.}}} t_{ij}^{ab} |\Phi_{ij}^{ab}\rangle. \tag{11}$$

The amplitudes t_{ij}^{ab} are obtained by solving a set of so-called double amplitude equations reading

$$\left\langle \Phi_{ij}^{ab} | e^{-\hat{T}} \hat{H} e^{\hat{T}} | \Phi \right\rangle = 0. \tag{12}$$

Solving equation (12) self-consistently for t_{ij}^{ab} leads to a resummation of infinitely many diagrams of a certain type. Removing all the terms from the above amplitude equation that do not correspond to so-called ring-diagrams defines the so-called ring-CCD.

Recently, the equivalence between direct i.e. 'Coulomb term only' ring-CCD (drCCD) and RPA as considered by Freeman [36], re-examined by Grüneis and Kresse [43] and Scuseria *et al* [6], was demonstrated. Scuseria *et al* algebraically showed that the CCD approximation to the many-electron wavefunction contains ring-approximation, i.e. the RPA to the ground-state correlation energy, but also includes selected higher-order exchange and ladder diagrams [36, 72, 73]. In other words, RPA equals drCCD and therefore corresponds to a subset of CCD diagrams.

Within the framework of CC expansions, the RPA and RPA + SOSEX correlation energies may be calculated using drCCD amplitudes $\{t_{ij}^{ab}\}$ by employing the respective equations [6, 36, 37]

$$E_c^{\text{RPA}} = \frac{1}{2} \sum_{ijab} B_{ia,jb}\, t_{ij}^{ab}, \tag{13}$$

$$E_c^{\text{RPA+SOSEX}} = \frac{1}{2} \sum_{ijab} K_{ia,jb}\, t_{ij}^{ab}. \tag{14}$$

The matrices $B_{ia,jb}$ and $K_{ia,jb}$ are of rank $N_{\text{occ}} \times N_{\text{virt}}$, and are defined by two-electron integrals $B_{ia,jb} = \langle ij \,|\, ab\rangle$ and $K_{ia,jb} = \langle ij \,|\, ab\rangle - \langle ij \,|\, ba\rangle$, respectively,

$$\langle pq|rs\rangle = \int\int \phi_p^*(\mathbf{x})\phi_r(\mathbf{x}) \frac{1}{|\mathbf{r}-\mathbf{r}'|} \phi_q^*(\mathbf{x}')\phi_s(\mathbf{x}')\mathrm{d}\mathbf{x}\,\mathrm{d}\mathbf{x}', \tag{15}$$

with $\mathbf{x} = \{\mathbf{r}, \sigma\}$. The amplitudes $\{t_{ij}^{ab}\}$ are obtained by solving a set of nonlinear Riccati equations, closely related to the time-dependent HF or more precisely the time-dependent Hartree method [6],

$$\begin{aligned} \langle ij|ab\rangle \quad & +(\varepsilon_c - \varepsilon_k)\delta_{ac}\delta_{ik} t_{kj}^{cb} + \langle ic|ak\rangle t_{kj}^{cb} \\ & + t_{ik}^{ac}(\varepsilon_c - \varepsilon_k)\delta_{bc}\delta_{jk} + t_{kj}^{cb}\langle ic|ak\rangle \\ & + t_{ik}^{ac}\langle kl|cd\rangle t_{lj}^{db} = 0. \end{aligned} \tag{16}$$

The previous equation can be rewritten in a more compact form [6],

$$\mathbf{B} + \mathbf{AT} + \mathbf{TA} + \mathbf{TBT} = 0, \tag{17}$$

with $A_{ia,jb} = (\epsilon_a - \epsilon_i)\delta_{ij}\delta_{ab} + \langle ib|aj\rangle$, $B_{ia,jb} = \langle ij|ab\rangle$ and $T_{ia,jb} = t_{ij}^{ab}$, underlining the quadratic order in the amplitudes' matrix $\mathbf{T}$.

Freeman has evaluated the RPA correlation energy of the unpolarized electron gas for various electron densities [36] using the drCCD equations and compared them to Hedin's RPA results (see table 2 in [79]) following an approach suggested by Nozières and Pines [80].

Both agree to within the numerical accuracy employed in the calculations. Moreover, Freeman has gone beyond RPA via the inclusion of the SOSEX diagram. He found that SOSEX reduces the correlation energy by about 30%. Monkhorst and Oddershede [81] came to similar conclusions employing RPA and RPA + SOSEX to metallic hydrogen, and Grüneis [37] observed a similar reduction of the correlation energy for small atoms finding good agreement with highly accurate CC correlation energies only after inclusion of SOSEX. Finally, we note that until recently the formulation of SOSEX within an ACFD framework has not been entirely clear, but has lately been shown by Jansen *et al* [82].

2.3. Single excitations and their renormalization

As alluded to above, in most practical calculations, RPA and SOSEX correlation energies are evaluated using KS orbitals from local or semilocal density functionals [3, 12] or GKS orbitals [7, 9, 17] from range-separated density functionals. This way, both RPA and SOSEX can be interpreted in terms of many-body perturbation theory (MBPT) based on a (generalized) KS reference state, where only a selected type of diagrams are summed up to infinite order. If one performs a simple Rayleigh–Schrödinger perturbation theory (RSPT) starting from an (approximate) KS-DFT reference, and examines the perturbation series at second order, one can identify a term arising from SEs which is not included in RPA or SOSEX correlation energies. In terms of single-particle orbitals, this term can be expressed as

$$E_c^{\mathrm{SE}} = \sum_{ia} \frac{|\langle i|v^{\mathrm{HF}} - v^{\mathrm{eff}}|a\rangle|^2}{\epsilon_i - \epsilon_a}, \tag{18}$$

where v^{HF} is the self-consistent HF potential, and v^{eff} is the effective single-particle potential that defines the non-interacting reference Hamiltonian h^{eff} giving rise to the single-particle orbitals $|i\rangle$ and $|a\rangle$ in the above expression. (See the supplementary material of [25] for a detailed derivation.) As is obvious from equation (18), E_c^{SE} trivially vanishes for the HF reference, i.e. when $v^{\mathrm{eff}} = v^{\mathrm{HF}}$, but is non-zero otherwise. It has been shown that adding this term to RPA significantly improves the description of weak interactions [25]. Note that the choice of v^{eff} in equation (18) is slightly different in RSPT from that in the second-order Görling–Levy perturbation theory (GL2) [83]. In the latter case, $v^{\mathrm{eff}} = v^{\mathrm{EXX-OEP}}$, with $v^{\mathrm{EXX-OEP}}$ being the EX OEP [52–54] potential. The difference between the two perturbation theories lies in the choice of the adiabatic-connection path (λ-integral)—in GL2 the electron density is kept fixed along the pathway and the perturbative Hamiltonian has a nonlinear dependence on λ, whereas in RSPT the λ-dependence of the perturbative Hamiltonian is linear, but the electron density varies along the λ-integral. Equation (18) in RSPT is more efficient and practically useful in the sense that there is no need to solve the computationally intensive and sometimes numerically problematic EXX-OEP equation and more flexible in the sense that it can be matched to any

suitable reference state. The price one has to pay is that the theory, strictly speaking, is not KS-DFT formulated within the ACFD framework.

The SE contribution at second order as given by equation (18) may become ill-behaved when the single-particle gap closes. To deal with this problem, in [25] a sequence of higher-order terms involving SE processes have been identified and summed up in the spirit of RPA. This leads to an 'rSE contribution' to the correlation energy,

$$E_c^{\mathrm{rSE}} = \sum_{ia} \frac{|\langle i|\Delta v|a\rangle|^2}{\epsilon_i - \epsilon_a + \langle i|\Delta v|i\rangle - \langle a|\Delta v|a\rangle}, \tag{19}$$

where $\Delta v = v^{\mathrm{HF}} - v^{\mathrm{eff}}$. The additional term $\langle i|\Delta v|i\rangle - \langle a|\Delta v|a\rangle$ in the denominator of equation (19) is negative definite, and prevents possible divergence of the expression even when the KS gap closes. The rSE correction is therefore expected to have a more general applicability, while preserving the good performance of the second-order SE for wide-gap molecules and insulators. In deriving equation (19), however, the 'non-diagonal' elements in the higher-order SE diagrams have been neglected for simplicity. Such an approach lacks invariance with respect to unitary transformations (orbital rotations) within the occupied and/or unoccupied subspaces. The orbital-rotation-invariance can be restored by including the 'non-diagonal' elements. This can be achieved by first semi-diagonalizing the Fock Hamiltonian $f = h^{\mathrm{eff}} + v^{\mathrm{HF}} - v^{\mathrm{eff}}$ separately within the occupied and unoccupied subspaces of h^{eff} and utilizing the resultant (so-called *semi-canonical*) orbitals and orbital energies in equation (18). A detailed description of this procedure will be presented in a forthcoming paper. However, we emphasize that the results presented in our paper are based on equation (19), but despite the lack of rotational invariance in the orbitals of this approach, the numerical results are only very slightly affected.

As also demonstrated in [25], the SE contributions to the correlation energy can be effectively accounted for to a large extent by replacing the non-self-consistent HF total energy computed using KS orbitals by its self-consistent counterpart. In this so-called hybrid-RPA scheme, the RPA correlation energy is still evaluated using KS orbitals, whereas the EX term is evaluated using HF orbitals. The same strategy can be applied to 'RPA + SOSEX' calculations. In this paper, we will benchmark the influence of SE contributions on the performance of RPA and SOSEX both by explicitly including the (r)SE corrections and in terms of the hybrid scheme.

As outlined by Ren *et al* in [25], rendering the energy functional stationary with respect to variations in the orbitals implies a zero correlation energy contribution stemming from SEs. This is well known as Brillouin's theorem. It will be demonstrated in this work that SE effects represent a non-negligible contribution to the correlation energy and consequently affect the results on thermochemistry and kinetics. In the field of quantum chemistry, effects induced by SEs are known as orbital-relaxation effects [84, 85]. Besides MBPT discussed above, the SE terms are present in the CC theory as well. In this context, Scuseria and Schaefer have shown that CCD employing optimized-orbitals (see [86]) gives results very close to CCSD. On the other hand, optimizing orbitals for CCSD calculations does not lead to significant improvement of the wavefunction. In other words, changes in the correlation energy induced upon inclusion of SEs may be effectively incorporated by means of a unitary transformation, i.e. rotation of the orbitals, as given in equation (6) of [86].

We close this section by presenting table 1, which summarizes the acronyms of the various methods applied in this work. For the KS single-determinant reference wave function we use the Perdew, Burke and Ernzerhof (PBE) [87] generalized gradient approximation (GGA).

Table 1. List of methods used throughout this work and their acronyms. Note that the total energy at the EX level is abbreviated as 'EX'.

(EX + RPA)@PBE	EX and RPA evaluated with a PBE reference, i.e. PBE orbitals and eigenvalues
HF + RPA @PBE	HF total energy combined with RPA using a PBE reference
(EX + RPA + SE)@PBE	EX and RPA augmented with SE using the PBE reference
(EX + RPA + rSE)@PBE	EX and RPA augmented with rSE using the PBE reference
HF + (RPA + SOSEX)@PBE	HF total energy combined with RPA + SOSEX using the PBE reference
(EX + RPA + SOSEX)@PBE	EX, RPA + SOSEX using the PBE reference
(EX + RPA + SOSEX + rSE) @PBE	EX, RPA + SOSEX and rSE using the PBE reference

We adopt the notation introduced by Ren *et al* in [17]; hence '@PBE' means 'evaluated using PBE orbitals and orbital energies'. This particular choice of orbitals is mainly driven by the following arguments: (i) PBE contains no empirically adjusted parameters, (ii) it performs slightly better than LDA (see e.g. [12]) and (iii) it is computationally less expensive to calculate the orbitals using semilocal functionals instead of e.g. hybrid functionals [17]. In addition, once one restricts the input orbitals to KS orbitals, results have shown to be virtually identical to those obtained using PBE orbitals [24, 88].

3. Computational details

Computational results of this work are based on calculations using (i) the Vienna *ab initio* simulation package (VASP) [89–91], (ii) a development version of the GAUSSIAN [92] suite of programs and (iii) FHI-aims [93, 94]. All of the software packages used have had the RPA and RPA + SOSEX functionals available since recently [7, 9, 12, 17]. VASP uses periodic boundary conditions and projector augmented plane waves as a basis set, which makes it ideally suited for extended, crystalline systems. GAUSSIAN is based on local, analytic Gaussian-type (GT) basis functions using open boundary conditions and the linear combination of atomic orbitals to expand the molecular orbitals. FHI-aims primarily uses numeric, atom-centered basis functions, but GT orbitals can be employed as well. In both cases, all the required integrals are evaluated numerically on an overlapping atom-centered grid [93]. The resolution-of-identity approximation is used to handle the four-centered Coulomb repulsion integrals and the KS response function (details of the implementation are presented in [94]). In this work, GT orbitals are used in FHI-aims calculations to facilitate a direct comparison with GAUSSIAN and the extrapolations to the complete basis set (CBS) limit.

In this work, we present statistical errors for the G2-1 set [44–47] as well as for BH6 [95], HTBH38/04 and NHTBH38/04 sets of 38 hydrogen transfer and 38 non-hydrogen transfer barrier heights after Zhao *et al* [48, 49]. Results for the molecular test sets use a two-point extrapolation procedure on the correlation energies to attain the CBS limit [96–98]. The chosen ansatz is motivated by an atomic partial wave expansion of the two-particle many-body wavefunction [97],

$$E_{\mathrm{corr}}^{X} = E_{\mathrm{corr}}^{\infty} + \frac{a}{X^3}, \tag{20}$$

where E_{corr}^{X} are correlation energies corresponding to the c.c.-pVXZ basis sets. For G2-1, CBS calculations are based on Dunning's correlation-consistent c.c.-pVQZ and c.c.-pV5Z basis

Table 2. Matching radii r_c of the PAW potentials used in the present work. If the matching radii differ for specific quantum numbers, they are specified for each l-quantum number using subscripts.

	Valence	r_c (a.u.)		Valence	r_c (a.u.)
H	1s	1.0_s 1.1_{pd}	F	2s2p	1.1_s 1.4_{pd}
Li	1s2s	1.2_s 1.5_{pd}	Mg	2p3s	2.0_{sd} 1.6_p
B	2s2p	1.5_s 1.7_{pd}	Al	3s3p	1.9_{spd} 2.0_f
C	2s2p	1.2_s 1.5_{pd}	Si	3s3p	1.5_s 1.9_{pd}
N	2s2p	1.3_s 1.5_{pd}	P	3s3p	1.9_{sp} 2.0_{df}
O	2s2p	1.2_s 1.5_{pd}	Cl	3s3p	1.7_s 1.9_{pdf}

sets [99, 100]. Note that throughout this work CBS extrapolation will be denoted by, e.g., c.c.-pV(Q,5)Z.

Moreover, G2-1 calculations employ the Boys–Bernardi counterpoise correction [101] to correct for basis set superposition errors (BSSE) within a particular basis set. Therefore, we emphasize that the CBS procedure uses BSSE-free correlation energies. In order to avoid inaccuracies from numerical quadrature of xc energy contributions, GAUSSIAN calculations use a grid of 400 radial shells and 770 angular points in each shell to converge the KS orbitals. GAUSSIAN employs a root-mean-square convergence criterion for the density matrix in the SCF iteration of 0.1 μHartree, which implies an energy convergence no worse than at least 0.01 μHartree (GAUSSIAN keyword: `SCF=tight`). In FHI-aims the grid setting '`tight`' together with '`radial_multiplier=6`' has been used to achieve convergence within 1 μHartree.

Results on barrier heights in BH6, HTBH38/04 and NHTBH38/04 use a c.c.-pV(T,Q)Z CBS extrapolation of the correlation energies and do not employ counterpoise corrections. To test for the errors incurred, we make a comparison with benchmark results obtained using RPA and RPA + SOSEX given in [9]. The statistical errors in barrier heights deviate from the aforementioned benchmark values by at most 1 kJ mol^{-1}. Hence, the errors incurred using smaller basis sets are minute and consequently are not expected to bias the conclusions.

The test set on atomization energies for crystalline solids includes 11 archetypal semiconductors and insulators. Specifically, it comprises C, Si, SiC, BN, BP, AlN, AlP, LiH, LiF, LiCl and MgO. The projector augmented wave (PAW) pseudopotentials (technical details in table 2) and kinetic energy cutoffs employed in the present calculations are identical to those used in [102]. Table 3 summarizes the lattice constants used in 'post-RPA' calculations. Moreover, we specify plane wave cutoffs for the overlap charge densities described in [38] and [102]. The SOSEX correlation energy was calculated using a $(3 \times 3 \times 3)$ Γ-centered k mesh, except for BN and BP due to a slower k-point convergence of the energy. For these systems a $(4 \times 4 \times 4)$ mesh was used. RPA correlation energies are taken from the literature (see [38]). In VASP, atoms are calculated using a supercell approach. The dimension of the supercells has been chosen as $(9 \times 9 \times 9)$ Å^3 in size. To reduce the computational cost of the 'RPA + SOSEX' calculations for isolated atoms, natural orbitals obtained using second-order perturbation theory have been employed. As outlined in [107], natural orbitals substantially improve convergence of the correlation energy with respect to the number of virtual orbitals.

To assess the codes used in this work, we compare numerical results obtained using the 'RPA' and 'RPA + SOSEX' implementations of GAUSSIAN and FHI-aims. Table 4 shows

Table 3. Experimental lattice constants, a^{exp}, extrapolated to 0 K. Energy cutoffs for the one-electron wave functions E_{PW} as well as energy cutoffs representing the overlap charge densities E_{χ} employed in the calculation of the atomization energies of solids. The corresponding structures are denoted using the Strukturbericht symbols in parentheses in the first column (A4 = diamond, B1 = rock-salt, B3 = zinc-blende). All energies and lattice constants are in eV and Å, respectively.

	a^{exp}	E_{PW}	E_{χ}
C (A4)	3.567[a]	550	400
Si (A4)	5.430[a]	450	300
SiC (B3)	4.358[a]	550	400
BN (B3)	3.607[b]	550	400
BP (B3)	4.538[b]	450	350
AlN (B3)	4.380[c]	550	400
AlP (B3)	5.460[b]	450	350
LiH (B1)	4.064[d]	600	450
LiF (B1)	4.010[a]	600	450
LiCl (B1)	5.106[a]	600	450
MgO (B1)	4.207[a]	600	450

[a] Staroverov *et al* [103].
[b] Madelung [104].
[c] Trampert *et al* [105].
[d] Smith and Leider [106].

Table 4. Benchmark calculations for atomic He using FHI-aims and GAUSSIAN and a c.c.-pV5Z GT orbital basis set. Results are given in Hartree atomic units.

He/c.c.-pV5Z	GAUSSIAN	FHI-aims
HF	−2.861 624 68	−2.861 624 83
MP2	−0.036 406 06	−0.036 406 51
RPA@HF	−0.065 244 88	−0.065 245 70
(RPA + SOSEX)@HF	−0.032 622 44	−0.032 622 85

correlation energies for the He atom obtained using the c.c.-pV5Z basis set. In order to avoid errors caused by numerical integration, we decided to use (restricted, i.e. spin-unpolarized) HF orbitals and eigenvalues for the calculation of RPA and RPA + SOSEX. The agreement found is close to perfect. Differences between the results are within a sub-micro-Hartree error margin. In passing we mention that FHI-aims employs the resolution-of-identity (RI) technique [94], which (i) reduces the computational workload significantly and (ii), as shown in table 4, does not sacrifice accuracy. For the molecular test sets, we always crosscheck the 'RPA' and 'RPA + SOSEX' results obtained with the GAUSSIAN suite of programs and FHI-aims to make sure that the results presented in this paper are not affected by actual implementations. 'SE' and 'rSE' have so far been implemented only in FHI-aims and we use these results throughout.

Table 5. MEs and MUEs in atomization or binding energies of 11 solids (see table 3) and 55 molecules (G2-1), in the barrier heights comprised in BH6, in HTBH38/04 (hydrogen transfer barriers), as well as in NHTBH38/04 (non-hydrogen transfer barriers). Results are given in kJ mol^{-1}.

	Solids		G2-1		BH6		HTBH38		NHTBH38	
Method	ME	MUE	ME	MUE	ME	MUE	ME	MUE	ME	MUE
(EX + RPA)@PBE	−67.5	67.5	−42.7	42.8[a]	1.2	7.5[a]	−0.8	7.1	−10.5	12.1
HF + RPA @PBE	−34.7	36.7	−25.3	30.3	−25.5	25.5	−36.8	36.8	−48.5	48.5
(EX + RPA + SE)@PBE			−14.2	22.9	−23.8	23.8	−52.7	52.7	−50.6	51.9
(EX + RPA + rSE)@PBE			−26.2	27.4	−14.8	16.3	−18.0	21.7	−31.4	31.4
(EX + RPA + SOSEX)@PBE	−27.0	27.0	−20.3	23.0[a]	17.6	17.6[a]	22.2	22.2	13.4	15.5
HF + (RPA + SOSEX)@PBE	5.8	17.4	−2.9	13.0	−9.2	9.2	−13.8	13.8	−24.7	25.5
(EX + RPA + SOSEX + rSE) @PBE			−4.0	13.9	3.1	3.7	3.6	5.4	−6.3	17.6

[a] See [9]. Note that differences in the MUE of G2-1 are due to the different values of the experimental dissociation energies (see [108]).

4. Results and discussion

The central findings of this work are summarized in table 5, presenting binding energies in molecules (G2-1) and solids, HT activation energies or barrier heights (BH6, HTBH38) as well as NHT barrier heights (NHTBH38). Whenever results are compared to experiment or to the best theoretical estimates, we use the mean error (ME) and mean unsigned error (MUE) as statistical measures to assess the accuracy of individual methods employed. Note that the experimental reference values are corrected for zero-point effects and are taken from the literature (G2-1: [108]; atomization energies in solids: [109]; barrier heights in BH6, HT/NHTBH38: [48, 95] and [49]). Reaction energies, as presented in table 6, are calculated from barrier heights in HTBH38 and NHTBH38, respectively.

4.1. Atomization energies of small molecules and solids

The notorious underbinding of (EX + RPA)@PBE in molecules and solids has already been demonstrated in many studies [3, 9, 12, 13, 17, 37, 38]. Table 5 presents MEs and MUEs in binding (atomization) energies obtained using (EX + RPA)@PBE for insulating solids (see section 3) as well as for the molecules contained in the G2-1 set. On average, (EX + RPA)@PBE underbinds solids compared to experiment by −67 kJ mol^{-1} (see also [38]) and molecules by −43 kJ mol^{-1}. We repeat that experimental binding energies are corrected for zero-point effects and are taken from the literature (for G2-1, see [108]; for the test set on solids, see [109] and references therein).

Following the suggestion of Ren *et al* [25], effects incurred by replacing the EX@PBE reference energy by the HF total energy have been checked for both molecules and solids. Indeed, HF + RPA @PBE improves binding energies of molecules *and* solids by almost 50% compared to (EX + RPA)@PBE. Figure 1 presents mean unsigned *relative* errors (MURE) in molecular (full bars) as well as solid state (squared bars) binding energies. Overall differences

Table 6. MEs and MUEs (kJ mol^{-1}) in the reaction energies obtained using calculated barrier heights of the HTBH38/04 hydrogen transfer as well as NHTBH38/04 non-hydrogen transfer barrier heights.

	HTBH38		NHTBH38	
Method	ME	MUE	ME	MUE
(EX + RPA)@PBE	−3.2	18.2	−7.8	9.7
HF + RPA @PBE	2.2	12.3	−1.6	14.4
(EX + RPA + SE)@PBE	−3.0	16.9	9.4	24.6
(EX + RPA + rSE)@PBE	−2.9	17.0	−1.2	11.8
(EX + RPA + SOSEX)@PBE	2.7	4.6	−18.4	20.5
HF + (RPA + SOSEX)@PBE	2.8	4.1	−12.2	15.7
(EX + RPA + SOSEX + rSE)@PBE	3.0	4.4	−11.9	15.5

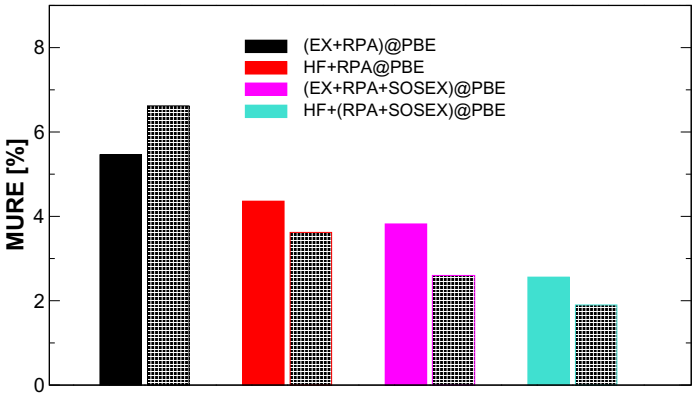

Figure 1. MURE in the atomization energies of 55 small molecules contained in G2-1 (full bars) and 11 insulating solids (squared bars) obtained using four of the RPA-based methods presented in this paper.

in MUREs are rather small. For the commonly applied (EX + RPA)@PBE method, the MURE is found to be approximately 6%. Using HF at the EX level reduces the MURE by more than 1%. It appears that the aforementioned improvements are less pronounced at the relative scale, and the error reduction is apparently bigger for solids than for molecules.

The explicit inclusion of the SE contribution to the correlation energy 'SE@PBE' obtained using equation (18) has been evaluated for molecules only. Adding 'SE@PBE' to (EX + RPA)@PBE leads to an ME of approximately −14 kJ mol^{-1} (see table 5) and an MUE of approximately 23 kJ mol^{-1}, clearly outperforming HF + RPA @PBE. Relative unsigned errors in G2-1 collected in figure 2 further corroborate the improvements of (EX + RPA + SE)@PBE over HF + RPA@PBE. Overall, these results confirm the findings presented by Ren *et al* in [25]. However, 'renormalization' of the SE contributions, as required for systems with a small one-electron band gap in PBE (see activation energies discussed in section 4.2), brings the atomization energies in the G2-1 test set back into almost perfect agreement with HF + RPA@PBE. Therefore, the good agreement with experiment

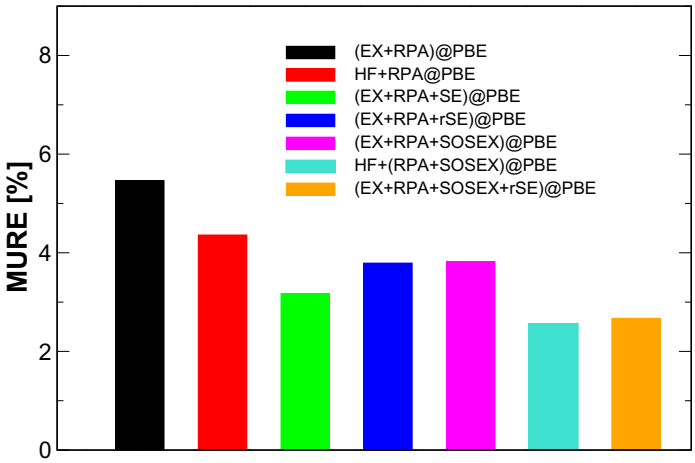

Figure 2. MURE (given in %) in G2-1 for all RPA-based methods presented in this paper. Atomization energies use counterpoise correction and correlation energies are CBS extrapolated using c.c.-pV(Q,5)Z.

for the G2-1 test set on the level of (EX + RPA + SE)@PBE is most likely to some extent fortuitous.

As extensively discussed in [37] and [9], the (RPA + SOSEX) correlation energy, here denoted as '(RPA + SOSEX)@PBE', represents a correction to (EX + RPA)@PBE rectifying the one-electron self-interaction error contained in 'RPA@PBE' due to exclusion principle violating diagrams [39]. Results for G2-1 obtained using (EX + RPA + SOSEX)@PBE are taken from [9] and included in table 5. The ME in G2-1 obtained using (EX + RPA + SOSEX)@PBE is approximately equal to $-20\,\mathrm{kJ\,mol^{-1}}$. For solids, the ME error reduces to $-27\,\mathrm{kJ\,mol^{-1}}$. Compared to (EX + RPA)@PBE, this represents substantial improvements of approximately 50% for atomization energies.

Given that both SOSEX and rSE, or alternatively replacing EX@PBE by HF, alleviate the tendency of (EX + RPA)@PBE to underbind, both schemes are expected to work cooperatively for the atomization energies of small molecules. Indeed, replacing 'EX@PBE' in (EX + RPA + SOSEX)@PBE by the HF total energy yields excellent results, with a slight underbinding for molecules (ME $= -2.9\,\mathrm{kJ\,mol^{-1}}$) and a slight overbinding for solids (ME $= 5.8\,\mathrm{kJ\,mol^{-1}}$). Again, the HF + (RPA + SOSEX)@PBE (ME $= -2.9\,\mathrm{kJ\,mol^{-1}}$) and the (EX + RPA + SOSEX + rSE)@PBE methods (ME $= -4.0\,\mathrm{kJ\,mol^{-1}}$) perform almost on par for molecules.

In summary, SE diagrams improve (EX + RPA)@PBE atomization energies of small molecules at virtually zero additional computational cost. However, as we will see below, this method fails when the one-electron band gaps in PBE become small. The better founded rSE does not perform equally well for atomization energies when combined with RPA. Combined with RPA + SOSEX it yields impressive atomization energies that are also in almost perfect agreement with the 'hybrid variants', e.g. the (self-consistent) HF total energy together with '(RPA + SOSEX)@PBE'. Overall, this indicates that (EX + RPA + SOSEX + rSE)@PBE or HF + (RPA + SOSEX)@PBE are the methods of choice for atomization energies.

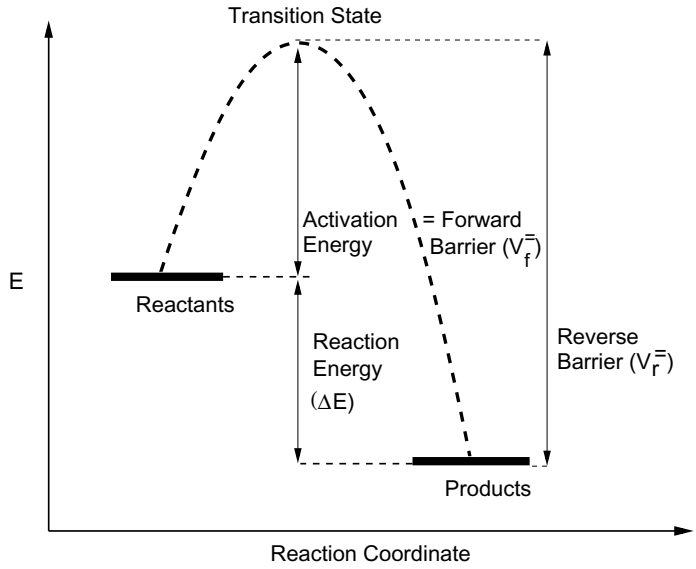

Figure 3. Schematic representation of activation and reaction energies.

4.2. Activation energies in HTBH38 and NHTBH38 chemical reactions

The ability to accurately describe the topology of multidimensional potential energy surfaces spanned by the internal molecular degrees of freedom, i.e. the reaction coordinates, in the course of a chemical reaction, is central to first-principles electronic structure methods. Calculating the energy difference between reactants and transition states (see figure 3) is a stringent test for the accuracy of density functionals. As mentioned in section 3, the HTBH38 and NHTBH38 test sets established by Truhlar and coworkers [48, 49] will be used here to test the RPA-based functionals considered.

Our findings on barrier heights, i.e. activation energies (figure 3), are summarized in table 5. MEs and MUEs are calculated with respect to the best theoretical estimates currently available for HT and NHT barrier heights given in [48] and [49], respectively. Furthermore, the MUREs in HT barriers (panel (a)) and NHT barriers (panel (b)) are depicted in figure 4. Note that legends given in figure 4 follow the color code used in figure 2. To establish a connection to [9], table 5 also shows MEs and MUEs for the BH6 test set [95], which has been introduced as a computationally less intensive, but statistically representative subset of HT/NHTBH38. However, we do not present a detailed discussion on BH6 here, but stress that errors in BH6 essentially follow the trends found for HT/NHTBH38.

One of the main findings of this work is the astonishingly good performance of the conventional (EX + RPA)@PBE scheme for activation energies. To be more specific, (EX + RPA)@PBE performs significantly better for the transfer of hydrogen atoms than for reactions involving heavier atoms. For HTBH38, the ME obtained using (EX + RPA)@PBE amounts to -0.8 kJ mol^{-1} and the associated MUE amounts to 7.1 kJ mol^{-1}. These error margins are similar to those of some of the range-separated, GKS-DFT functionals such as e.g. LC-ωPBE [110]. The latter performs very well for chemical reaction barriers (see also section 4.4). However, for (EX + RPA)@PBE, the MUE increases by more than 50% when elements heavier than H, such as e.g. F or Cl, are transferred. The MUE in NHTBH38 obtained using (EX + RPA)@PBE

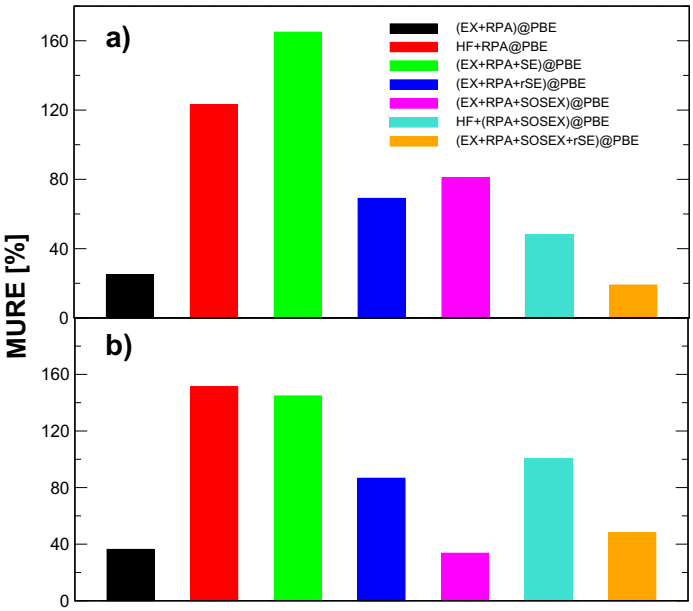

Figure 4. (a) MURE in HT barrier heights of HTBH38; (b) MUREs in NHTBH38 for the RPA-based methods presented in this work. Energies use a c.c.-pV(T,Q)Z extrapolation and the frozen core approximation in calculated correlation energies.

amounts to 12.1 kJ mol^{-1} together with a rather distinct underestimation of the barriers by −10.5 kJ mol^{-1} (ME).

On a relative scale, the MURE for HT reactions obtained using (EX + RPA)@PBE (see figure 4) amounts to approximately 20%, but increases to a value approximately twice as large for NHT reactions (panel (b)). Note that reaction number 7 in NHTBH38 has a barrier height of only −1.42 kJ mol^{-1}. For this reaction MUREs are extraordinarily large, leading to an increase that is seven to eight times as large as the corresponding value in HT reactions. The statistics would be drastically biased by such a case, being very likely compensated by significantly extending the test set. Therefore, we decided to exclude reaction number 7 from the test set when calculating the MURE in NHTBH38.

Both HF + RPA @PBE and (EX + RPA + SE)@PBE show a strong underestimation of barriers with maximal errors as large as 50 kJ mol^{-1}. As mentioned above, the reason for this behavior has been attributed to small HOMO-LUMO differences found for some of the transition state structures, which are not correctly described by the simple (EX + RPA + SE)@PBE scheme. Indeed, the renormalization of SE alleviates the problem, and the corresponding ME and MUE in HTBH38 obtained using (EX + RPA + rSE)@PBE are improved by almost 60% compared to (EX + RPA + SE)@PBE. Note that numerical results given in table 5 nicely reflect the trend induced by incorporation of SE effects in the correlation energy contribution, i.e. it partially takes care of the lack of self-consistency in the EX@PBE energy. However, the rSE corrects for the strong underestimation of barriers seen in HF + RPA @PBE and (EX + RPA + SE)@PBE, but qualitatively reflects the same trend compared to (EX + RPA)@PBE.

The performance of (EX + RPA + SOSEX)@PBE for barrier heights has already been tested by Paier *et al* for the BH6 test set [9]. This work extends the findings of [9] by

discriminating between HT and NHT reactions. (EX + RPA + SOSEX)@PBE is less accurate for HT barriers than (EX + RPA)@PBE, as indicated by an MUE of about 22 kJ mol^{-1} compared to 7 kJ mol^{-1}. Quantitatively, (EX + RPA + SOSEX)@PBE on average overestimates barrier heights for HTBH38 by the aforementioned 22 kJ mol^{-1}. This is in perfect agreement with the errors found for the BH6 test set [9]. On the other hand, (EX + RPA + SOSEX)@PBE performs substantially better for NHT barrier heights, where ME and MUE are found to be close to those obtained using (EX + RPA)@PBE. On average, (EX + RPA + SOSEX)@PBE overestimates NHT barriers by approximately 13 kJ mol^{-1}, whereas (EX + RPA)@PBE underestimates them by 11 kJ mol^{-1}. As shown in figure 4, the MURE in NHT barriers obtained using (EX + RPA + SOSEX)@PBE amounts to 34% (panel (b) in figure 4), slightly outperforming (EX + RPA)@PBE by approximately 3%.

Incorporation of SE effects into (EX + RPA + SOSEX)@PBE in the hybrid fashion, i.e. HF + (RPA + SOSEX)@PBE, leads to very different results when applied to HT and NHT reactions, respectively. HF + (RPA + SOSEX)@PBE improves HT reaction barrier heights, whereas NHT barrier heights deteriorate appreciably compared to (EX + RPA + SOSEX)@PBE, ending up with an overall underestimation of barrier heights.

The situation becomes noticeably better, for both HT and NHT barrier heights, upon combination of explicitly computed rSE with (EX + RPA + SOSEX)@PBE. Barrier heights obtained using (EX + RPA + SOSEX + rSE)@PBE are of similar quality to 'conventional' (EX + RPA)@PBE, although the unsigned error in the NHT test set is slightly larger. (EX + RPA + SOSEX + rSE)@PBE overestimates HT barriers by approximately 3.6 kJ mol^{-1}, but reduces the ME in NHT barriers (ME $-$ 6.3 kJ mol^{-1}) compared to (EX + RPA)@PBE.

To summarize this section, SOSEX and rSE tend to overestimate and underestimate reaction barrier heights, respectively. Thus it appears advantageous to combine the correction schemes in order to achieve a partial error compensation. This mechanism works most efficiently for HT reactions and somewhat less so for NHT reactions. Taking the excellent performance of (EX + RPA + SOSEX + rSE)@PBE for binding energies (see the previous section) into account, this functional offers the most balanced description in terms of binding energies as well as activation energies.

4.3. Reaction energies in HTBH38 and NHTBH38

As shown in figure 3, knowing both forward ($V_f^{\neq}$) and reverse ($V_r^{\neq}$) reaction barrier heights, corresponding reaction energies ΔE are readily calculated using

$$\Delta E = V_f^{\neq} - V_r^{\neq}. \tag{21}$$

Note that 17 out of the 38 reactions contained in HTBH38 lead to a nonzero ΔE, whereas NHTBH38 comprises 13 reactions with a forward barrier different from the reverse barrier. The corresponding MEs and MUEs of the RPA-based functionals are compiled in table 6, and the MUREs are depicted in figure 5.

Similar to the trends found for atomization energies, HT reaction energies are significantly improved upon inclusion of (SOSEX)@PBE to (EX + RPA)@PBE as reflected in the MUEs. For (EX + RPA)@PBE the MUE in HT reactions amounts to 18.2 kJ mol^{-1} and drops down to 4.6 kJ mol^{-1} employing (EX + RPA + SOSEX)@PBE. Hence, it appears that eliminating the one-electron self-correlation error contained in RPA@PBE is beneficial for HT reaction energies. This is not entirely surprising, since the aforementioned error will be largest for

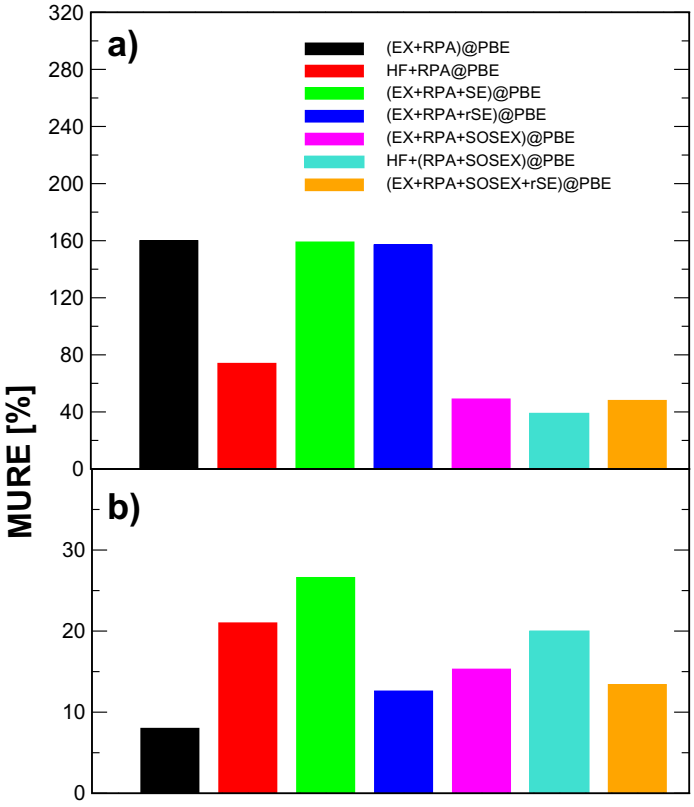

Figure 5. (a) Shows MURE in HT reaction energies of HTBH38; (b) shows MURE for the reaction energies of NHTBH38. Energies use a c.c.-pV(T,Q)Z extrapolation and the frozen core approximation to the correlation energies. The color code of legends follows figure 4.

breaking and creating covalent hydrogen bonds. For reactions involving heavier atoms, as exemplified by the reaction energies in NHTBH38, the correction due to (SOSEX)@PBE appears to perform less favorably. This can be seen by inspection of figure 5 presenting MUREs in HT (panel (a)) as well as NHT reaction energies (panel (b)). For (EX + RPA)@PBE the MUE in NHTBH38 amounts to 9.7 kJ mol^{-1}, which is rather low, whereas for NHT reaction energies obtained using (EX + RPA + SOSEX)@PBE, the MUE increases to 20.5 kJ mol^{-1}.

Concerning effects due to SE@PBE and rSE@PBE to (EX + RPA)@PBE, no significant improvement of HT reaction energies over (EX + RPA)@PBE has been found. The MEs and MUEs given in table 6 for (EX + RPA + SE)@PBE (ME $-$ 3 kJ mol^{-1}; MUE = 16.9 kJ mol^{-1}) and (EX + RPA + rSE)@PBE (ME = $-$2.9 kJ mol^{-1}; MUE = 17 kJ mol^{-1}) are essentially unaltered compared to (EX + RPA)@PBE. In contrast to HT, the rSE correction helps to improve the NHTBH38 reaction energies and alleviates the overestimation found for simple (EX + RPA + SE)@PBE drastically (ME = $-$1.2 kJ mol^{-1} compared to 9.4 kJ mol^{-1}). The associated MUE as well as MURE decrease by approximately 50%.

We now turn to a discussion of results obtained using the 'hybrid variants', which employ the HF energy as the reference energy on the EX level. Specifically for (EX + RPA)@PBE, HT reaction energies are substantially improved upon replacement of EX@PBE through HF. As can be seen from table 6, the MUE is reduced by approximately 6 kJ mol^{-1}, which

Table 7. Comparing the three best-performing functionals presented in table 5 to widely used semilocal and HF/DFT hybrid functionals. Mean unsigned errors in individual test sets are given in kJ mol^{-1}.

Method	G2-1	BH6	HTBH38	NHTBH38
(EX + RPA)@PBE	42.8[a]	7.5[a]	7.1	12.1
HF + (RPA + SOSEX)@PBE	13.0	9.2	13.8	25.5
(EX + RPA + SOSEX + rSE)@PBE	13.9	3.7	5.4	17.6
PBE	36.0[b]	38.9[c]	39.0[d]	33.9[d]
BLYP	19.7[b]	32.6[c]	31.5[d]	36.4[d]
PBE0	14.6[b]	19.2[c]	17.7[d]	14.1[d]
B3LYP	10.0[b]	19.7[c]	17.7[d]	18.2[d]
LC-ωPBE	15.6[e]		5.4[e]	10.0[e]

[a] See [9]. Note that differences in the MUE of G2-1 are due to the different values of the experimental dissociation energies (see [108]).
[b] Ernzerhof and Scuseria [111].
[c] Yang *et al* [112].
[d] Zhao *et al* [49].
[e] Vydrov and Scuseria [110]. Note that the MUE given here for G2 refers to G2-2 comprising 148 molecules. The MUE for G2-1 will be lower.

translates into an improvement of the MURE by approximately 50%. HT reaction energies obtained using (EX + RPA + SOSEX)@PBE, which are fairly accurate, are hardly affected by changing to the corresponding hybrid scheme. Employing HF + (RPA + SOSEX)@PBE, however, the MUE in NHT reaction energies is reduced by 5 kJ mol^{-1}. In addition, the ME amounts to -12 kJ mol^{-1}, which compares very favorably to the ME of -18 kJ mol^{-1} obtained using (EX + RPA + SOSEX)@PBE. In terms of performance, the combined scheme (EX + RPA + SOSEX + rSE)@PBE is on par with HF + (RPA + SOSEX)@PBE for both HTBH38 and NHTBH38 reaction energies.

(EX + RPA + SOSEX + rSE)@PBE has two apparently favorable features: (i) it substantially improves HT reaction energies obtained using (EX + RPA)@PBE and (ii) it performs approximately similarly well for *all* of the test sets investigated in this work. In other words, the overall variation in error margins for atomization energies, barrier heights and reaction energies is smallest for (EX + RPA + SOSEX + rSE)@PBE lending the functional robustness. Among the functionals discussed in this work, (EX + RPA)@PBE performs best for NHT reaction energies. Nevertheless, (EX + RPA + SOSEX + rSE)@PBE performs only slightly worse, but given the better HT reaction barrier heights and the significantly better reaction energies in HTBH38, (EX + RPA + SOSEX + rSE)@PBE is among the RPA-based functionals tested in this work, the functional of broadest applicability.

4.4. Comparison of RPA to semilocal and hybrid functionals

To close the discussion on the performance of the RPA- and RPA + SOSEX-based functionals, we briefly compare molecular atomization and activation energies to results obtained using commonly applied semilocal as well as HF/DFT hybrid functionals. To render direct comparisons easier, table 7 repeats MUEs for G2-1, BH6, HTBH38 and NHTBH38 for three

of the RPA-based functionals which perform best, namely (EX + RPA)@PBE, HF + (RPA + SOSEX)@PBE and (EX + RPA + SOSEX + rSE)@PBE. The above-mentioned statistical errors are compared to PBE-GGA, BLYP-GGA [113, 114] as well as the PBE0 [111, 115] and B3LYP [116] global hybrid functionals. In addition, we also present results obtained using the above-mentioned LC-ωPBE range-separated hybrid functional [110]. LC-ωPBE mixes a fraction of EX at the long range of the Coulomb interaction (for definitions, see [110]), but uses only one parameter (0.40 bohr^{-1}) to define a universal range separation. It is remarkable that LC-ωPBE describes reaction barriers and atomization energies extremely accurately, representing a landmark among hybrids for thermochemistry and kinetics. Admittedly, for extended systems, admixture of EX on the long range is detrimental and leads to e.g. strongly overestimated band gaps [117].

Returning to RPA, activation energies obtained using (EX + RPA)@PBE are *de facto* on a par with LC-ωPBE (table 7). Trends for GGA and global hybrid functionals like PBE0 or B3LYP are rather general; hence, other GGA-type and global hybrid functionals perform quite similarly (for other functionals, see, e.g., [112]). Although HF + (RPA + SOSEX)@PBE does not perform as well as (EX + RPA)@PBE for activation energies of non-hydrogen transfer reactions (corresponding MUE is almost twice as large), it certainly performs better than PBE and BLYP. HF + (RPA + SOSEX)@PBE is only slightly outperformed by B3LYP for the aforementioned activation energies in NHTBH38. According to this synopsis, (EX + RPA + SOSEX + rSE)@PBE certainly shows the most balanced description of molecular binding and barrier heights. It performs as well as hybrid functionals in terms of atomization energies, outperforms both GGA and hybrid functionals in terms of hydrogen-transfer barrier heights and performs equivalently well for non-hydrogen barrier heights as the aforementioned hybrids do.

Although this work is not devoted to weak, vdW-type interactions, it should be emphasized that all of the RPA-based functionals presented here do include them seamlessly as already mentioned in the introduction. It is well known that neither GGA nor hybrid functionals show the correct vdW asymptote.

5. Conclusions

In summary, we have reported an extensive assessment of several EX-based post-KS density functionals involving RPA correlation energies and beyond. Correlation energies have been assessed for solids as well as for small molecules. Specifically, we calculated atomization energies of solids and molecules using (EX + RPA)@PBE, (EX + RPA + SOSEX)@PBE as well as HF + RPA @PBE and HF + (RPA + SOSEX)@PBE, where the latter approach gives binding energies improved by approximately 50% compared to 'conventional' (EX + RPA)@PBE. Furthermore, we investigated the performance of individual functionals for chemical reaction barrier heights or activation energies employing large and well-established test sets. Generally, we found that it is rather difficult to systematically improve on (EX + RPA)@PBE reaction barrier heights, although modest improvements using (EX + RPA + SOSEX + rSE)@PBE were achieved for HT barriers. Importantly, the favorable impact of the correlation energy contribution stemming from SE effects on binding energies does not translate into reaction barriers. This has been explained by divergent correlation energy contributions in systems with small HOMO–LUMO gaps. Therefore, the application of 'SE' to systems with small one-electron band gaps is not possible, but a renormalization of 'SE' helps to alleviate the

problem. Surprisingly, (EX + RPA)@PBE yields reaction energies of high accuracy for reactions involving non-hydrogen atoms. Good and robust performance of a novel RPA-based functional (EX + RPA + SOSEX + rSE)@PBE is a central finding of this work. It improves on binding or atomization energies compared to (EX + RPA)@PBE, improves on HT barrier heights as well as reaction energies.

Acknowledgments

This work was supported by the Austrian Fonds zur Förderung der wissenschaftlichen Forschung (FWF) within SFB ViCom (F41). The work at Rice University was supported by the US Department of Energy (grant no. DE-FG02-09ER16053) and the Welch Foundation (C-0036).

References

[1] Bohm D and Pines D 1953 *Phys. Rev.* **92** 609
[2] Gell-Mann M and Brueckner K A 1957 *Phys. Rev.* **106** 364
[3] Furche F 2001 *Phys. Rev.* B **64** 195120
[4] Fuchs M and Gonze X 2002 *Phys. Rev.* B **65** 235109
[5] Furche F and Van Voorhis T 2005 *J. Chem. Phys.* **122** 164106
[6] Scuseria G E, Henderson T M and Sorensen D C 2008 *J. Chem. Phys.* **129** 231101
[7] Janesko B G, Henderson T M and Scuseria G E 2009 *J. Chem. Phys.* **130** 081105
[8] Toulouse J, Gerber I C, Jansen G, Savin A and Ángyán J G 2009 *Phys. Rev. Lett.* **102** 096404
[9] Paier J, Janesko B G, Henderson T M, Scuseria G E, Grüneis A and Kresse G 2010 *J. Chem. Phys.* **132** 094103
Paier J, Janesko B G, Henderson T M, Scuseria G E, Grüneis A and Kresse G 2010 *J. Chem. Phys.* **133** 179902 (erratum)
[10] Marini A, García-González P and Rubio A 2006 *Phys. Rev. Lett.* **96** 136404
[11] Jiang H and Engel E 2007 *J. Chem. Phys.* **127** 184108
[12] Harl J and Kresse G 2008 *Phys. Rev.* B **77** 045136
[13] Harl J and Kresse G 2009 *Phys. Rev. Lett.* **103** 056401
[14] Lu D, Li Y, Rocca D and Galli G 2009 *Phys. Rev. Lett.* **102** 206411
[15] Dobson J F and Wang J 1999 *Phys. Rev. Lett.* **82** 2123
[16] Rohlfing M and Bredow T 2008 *Phys. Rev. Lett.* **101** 266106
[17] Ren X, Rinke P and Scheffler M 2009 *Phys. Rev.* B **80** 045402
[18] Schimka L, Harl J, Stroppa A, Grüneis A, Marsman M, Mittendorfer F and Kresse G 2010 *Nature Mater.* **9** 741
[19] Zhu W, Toulouse J, Savin A and Ángyán J G 2010 *J. Chem. Phys.* **132** 244108
[20] Lebègue S, Harl J, Gould T, Ángyán J G, Kresse G and Dobson J F 2010 *Phys. Rev. Lett.* **105** 196401
[21] Eshuis H, Yarkony J and Furche F 2010 *J. Chem. Phys.* **132** 234114
[22] Ismail-Beigi S 2010 *Phys. Rev.* B **81** 195126
[23] Göltl F and Hafner J 2011 *J. Chem. Phys.* **134** 064102
[24] Eshuis H and Furche F 2011 *J. Phys. Chem. Lett.* **2** 983
[25] Ren X, Tkatchenko A, Rinke P and Scheffler M 2011 *Phys. Rev. Lett.* **106** 153003
[26] Heßelmann A and Görling A 2011 *Phys. Rev. Lett.* **106** 093001
[27] Heßelmann A and Görling A 2011 *Mol. Phys.* **109** 2473
[28] Ruzsinszky A, Perdew J P and Csonka G I 2011 *J. Chem. Phys.* **134** 114110
[29] Heßelmann A 2011 *J. Chem. Phys.* **134** 204107
[30] Klopper W, Teale A M, Coriani S, Pedersen T B and Helgaker T 2011 *Chem. Phys. Lett.* **510** 147

[31] Dobson J F 1994 *Topics in Condensed Matter Physics* ed M P Das (New York: Nova Science)
[32] Møller C and Plesset M S 1934 *Phys. Rev.* **46** 618
[33] Becke A D 1993 *J. Chem. Phys.* **98** 1372
[34] Becke A D 1993 *J. Chem. Phys.* **98** 5648
[35] Perdew J P, Ernzerhof M and Burke K 1996 *J. Chem. Phys.* **105** 9982
[36] Freeman D L 1977 *Phys. Rev.* B **15** 5512
[37] Grüneis A, Marsman M, Harl J, Schimka L and Kresse G 2009 *J. Chem. Phys.* **131** 154115
[38] Harl J, Schimka L and Kresse G 2010 *Phys. Rev.* B **81** 115126
[39] Henderson T M and Scuseria G E 2010 *Mol. Phys.* **108** 2511
[40] Ruzsinszky A, Perdew J P, Csonka G I, Vydrov O A and Scuseria G E 2006 *J. Chem. Phys.* **125** 194112
[41] Mori-Sánchez P and Cohen A J 2006 *J. Chem. Phys.* **125** 201102
[42] Hu C D and Langreth D C 1986 *Phys. Rev.* B **33** 943
[43] Kresse G and Grüneis A 2008 unpublished results, presented at the *XIV ESCMQC, (Isola d'Elba, Italy, 3 October, 2008)*
[44] Curtiss L A, Raghavachari K, Redfern P and Pople J 1997 *J. Chem. Phys.* **106** 1063
[45] Pople J A, Head-Gordon M, Fox D J, Raghavachari K and Curtiss L A 1989 *J. Chem. Phys.* **90** 5622
[46] Curtiss L A, Jones C, Trucks G W, Raghavachari K and Pople J A 1989 *J. Chem. Phys.* **93** 2537
[47] Curtiss L A, Redfern P C, Raghavachari K and Pople J A 1998 *J. Chem. Phys.* **109** 42
[48] Zhao Y, Lynch B J and Truhlar D G 2004 *J. Phys. Chem.* A **108** 2715
[49] Zhao Y, Gonzáles-García N and Truhlar D G 2005 *J. Phys. Chem.* A **109** 2012
Zhao Y, Gonzáles-García N and Truhlar D G 2006 *J. Phys. Chem.* A **110** 4942(E)
[50] Janesko B G and Scuseria G E 2008 *J. Chem. Phys.* **128** 244112
[51] Seidl A, Görling A, Vogl P, Majewski J A and Levy M 1996 *Phys. Rev.* B **53** 3764
[52] Sharp R T and Horton G K 1953 *Phys. Rev.* **90** 317
[53] Talman J D and Shadwick W F 1976 *Phys. Rev.* A **14** 36
[54] Casida M E 1995 *Phys. Rev.* A **51** 2005
[55] Szabo A and Ostlund N S 1996 *Modern Quantum Chemistry* 1st edn (New York: Dover)
[56] Dreizler R M and Gross E K U 1995 *Density Functional Theory* (New York: Plenum)
[57] Godby R W, Schlüter M and Sham L J 1986 *Phys. Rev. Lett.* **56** 2415
[58] Godby R W, Schlüter M and Sham L J 1988 *Phys. Rev.* B **37** 10159
[59] Kotani T 1998 *J. Phys.: Condens. Matter* **10** 9241
[60] Grüning M, Marini A and Rubio A *Phys. Rev.* B **74** 161103
[61] Hellgren M and von Barth U 2007 *Phys. Rev.* B **76** 075107
[62] Hellgren M, Rohr D R and Gross E K U 2012 *J. Chem. Phys.* **136** 034106
[63] Langreth D C and Perdew J P 1975 *Solid State Commun.* **17** 1425
[64] Gunnarsson O and Lundqvist B I 1976 *Phys. Rev.* B **13** 4274
[65] Langreth D C and Perdew J P 1977 *Phys. Rev.* B **15** 2884
[66] Gross E K U and Kohn W 1985 *Phys. Rev. Lett.* **55** 2850
[67] Onida G, Reining L and Rubio A 2002 *Rev. Mod. Phys.* **74** 601
[68] Harris F E, Monkhorst H J and Freeman D L 1992 *Algebraic and Diagrammatic Methods in Many-Fermion Theory* (Oxford: Oxford University Press)
[69] Brandow B H 1967 *Rev. Mod. Phys.* **39** 771
[70] Bartlett R J and Musiał M 2007 *Rev. Mod. Phys.* **79** 291
[71] Kümmel H, Lührmann K H and Zabolitzky J G 1978 *Phys. Rep.* **36** 1
[72] Bishop R F and Lührmann K H 1978 *Phys. Rev.* B **17** 3757
[73] Bishop R F and Lührmann K H 1982 *Phys. Rev.* B **26** 5523
[74] Čížek J 1966 *J. Chem. Phys.* **45** 4256
[75] Čížek J 1969 *Adv. Chem. Phys.* **14** 35
[76] Paldus J, Čížek J and Shavitt I 1972 *Phys. Rev.* A **5** 50

[77] Bartlett R J and Purvis G D III 1978 *Int. J. Quantum Chem.* **14** 561
[78] Bartlett R J 1981 *Annu. Rev. Phys. Chem.* **32** 359
[79] Hedin L 1965 *Phys. Rev.* **139** A796
[80] Nozières P and Pines D 1958 *Nuovo Cimento* **9** 470
[81] Monkhorst H J and Oddershede J 1973 *Phys. Rev. Lett.* **30** 797
[82] Jansen G, Liu R-F and Ángyán J G 2010 *J. Chem. Phys.* **133** 154106
[83] Görling A and Levy M 1993 *Phys. Rev.* B **47** 13105
[84] Raffenetti R C, Ruedenberg K, Janssen C L and Schaefer H F 1992 *Theor. Chim. Acta* **86** 149
[85] Ruedenberg K, Cheung L M and Elbert S T 1976 *Int. J. Quantum Chem.* **16** 1069
[86] Scuseria G E and Schaefer H F 1987 *Chem. Phys. Lett.* **142** 354
[87] Perdew J P, Burke K and Ernzerhof M 1996 *Phys. Rev. Lett.* **77** 3865
Perdew J P, Burke K and Ernzerhof M 1997 *Phys. Rev. Lett.* **78** 1396 (erratum)
[88] Eshuis H, Bates J E and Furche F 2012 *Theor. Chem. Acc.* **131** 1084
[89] Kresse G and Hafner J 1993 *Phys. Rev.* B **48** 13115
[90] Kresse G and Furthmüller J 1996 *Phys. Rev.* B **54** 11169
[91] Kresse G and Furthmüller J 1996 *Comput. Mater. Sci.* **6** 15
[92] Frisch M J *et al* 2007 *Gaussian Development Version Revision G.01* (Wallingford, CT: Gaussian)
[93] Blum V, Gehrke R, Hanke F, Havu P, Havu V, Ren X, Reuter K and Scheffler M 2009 *Comput. Phys. Commun.* **180** 2175
[94] Ren X, Rinke P, Blum V, Wieferink J, Tkatchenko A, Sanfilippo A, Reuter K and Scheffler M to be published
[95] Lynch B J and Truhlar D G 2003 *J. Phys. Chem.* A **107** 8996
Lynch B J and Truhlar D G 2004 *J. Phys. Chem.* A **108** 1460(E)
[96] Kutzelnigg W and Morgan J D III 1992 *J. Chem. Phys.* **96** 4484
[97] Helgaker T, Klopper W, Koch H and Noga J 1997 *J. Chem. Phys.* **106** 9639
[98] Halkier A, Helgaker T, Jørgensen P, Klopper W, Koch H, Olsen J and Wilson A K 1998 *Chem. Phys. Lett.* **286** 243
[99] Dunning T H Jr 1989 *J. Chem. Phys.* **90** 1007
[100] Woon D E and Dunning T H Jr 1993 *J. Chem. Phys.* **98** 1358
[101] Boys S F and Bernardi F 1970 *Mol. Phys.* **19** 553
[102] Grüneis A, Marsman M and Kresse G 2010 *J. Chem. Phys.* **133** 074107
[103] Staroverov V N, Scuseria G E, Tao J and Perdew J P 2004 *Phys. Rev.* B **69** 075102
[104] Madelung O 2004 *Semiconductors: Data Handbook* 3rd edn (Berlin: Springer)
[105] Trampert A, Brandt O and Ploog K 1998 *Crystal Structure of Group III Nitrides Semiconductors and Semimetals* vol 5 ed J I Pankove and T D Moustakas (San Diego, CA: Academic)
[106] Smith D K and Leider H R 1968 *J. Appl. Cryst.* **1** 246
[107] Grüneis A, Booth G H, Marsman M, Spencer J, Alavi A and Kresse G 2011 *J. Chem. Theory Comput.* **7** 2780
[108] Feller D and Peterson K A 1999 *J. Chem. Phys.* **110** 8384
[109] Schimka L, Harl J and Kresse G 2011 *J. Chem. Phys.* **134** 024116
[110] Vydrov O and Scuseria G E 2006 *J. Chem. Phys.* **125** 234109
[111] Ernzerhof M and Scuseria G E 1999 *J. Chem. Phys.* **110** 5029
[112] Yang K, Zheng J, Zhao Y and Truhlar D G 2010 *J. Chem. Phys.* **132** 164117
[113] Becke A D 1988 *Phys. Rev.* A **38** 3098
[114] Lee C, Yang W and Parr R G 1988 *Phys. Rev.* B **37** 785
[115] Adamo C and Barone V 1999 *J. Chem. Phys.* **110** 6158
[116] Stephens P J, Devlin F J, Chabalowski C F and Frisch M J 1994 *J. Phys. Chem.* **98** 11623
[117] Gerber I C, Ángyán J G, Marsman M and Kresse G 2007 *J. Chem. Phys.* **127** 054101